ONR TECHNICAL REPORT NO. 56

LIGHT SCATTERING STUDIES OF THE INTERNAL STRUCTURE OF FILMS AND FIBERS

January, 1963

MARION B. RHODES and RICHARD S. STEIN
POLYMER RESEARCH INSTITUTE
University of Massachusetts, Amherst, Massachusetts

LIGHT SCATTERING STUDIES OF THE INTERNAL STRUCTURE OF FIBERS AND FILMS[+]

Marion B. Rhodes and Richard S. Stein

POLYMER RESEARCH INSTITUTE
University of Massachusetts

Amherst, Mass.

INTRODUCTION

The use of light scattering for studying the structure of polycrystalline polymer films has been described by this and other laboratories and has been reviewed.[1,2,3] Theory and experimental methods for photographically and photometrically studying the scattering of films have been described. In this paper, currently used techniques and procedures for measuring the scattering of both films and fibers are described and methods for separating contributions to scattering from density and orientation heterogeneities and voids are proposed. Procedures are given for determining uniaxial and biaxial orientation of superstructure, as are methods for estimating sizes and anisotropy of structure.

PHOTOGRAPHIC METHODS FOR FILMS

A relatively simple photographic set-up suffices for low angle measurements (Fig. 1).[4,5] A parallel light beam is provided from a mercury arc, pinhole and lens arrangement. This is polarized with a polaroid sheet and passed normally through the sample. It then passes normally through an analyzing polaroid and finally on a photographic film (Ansco Super-Hypan or Polaroid). The relative orientation of polarizer and analyzer is designated as V_V when their polarization directions are parallel and H_V when they are perpendicular. Typical V_V and H_V patterns for medium density polyethylene are shown in Fig. 2.

[+]Supported in part by grants from the Chemstrand Research Center and the Petroleum Research Fund, and by contracts with the Office of Naval Research and the Atomic Energy Commission.

To avoid contribution from scattering from surface irregularities, films are held between glass microscope slides using an immersion fluid such as a silicone oil which closely matches the refractive index of the polymer but which does not swell the polymer. This procedure is essentially as can be seen in Fig. 3 showing scattering from a Teflon film without and with a well matched immersion fluid. The "propeller" type pattern in (3a) results from an oriented surface growth of crystalline superstructure which obscures the internal structure seen in the immersed samples in (3b).

It is also essential that the film be sufficiently thin to avoid distortion of the scattering pattern by secondary scattering. This may mean that films must be of the order of 1 mil thick for highly scattering samples but can be considerably thicker for samples of low turbidity. For example, Fig. 4 shows scattering patterns for thin and thick samples of a medium density polyethylene.

It is also important that optical surfaces be well aligned parallel to each other and perpendicular to the light beam to avoid spurious reflections of the type shown in Fig. 5.

Recently, a laser light source has been employed in these experiments[6] as shown in Fig. 6. A relatively low power laser (for example, Maser Optics Model 600) can reduce exposure times from hours to fractions of a second. The laser provides a parallel, monochromatic, polarized light beam directly, eliminating the need for auxiliary optical elements except for a guard pinhole to exclude fluorescence from the laser crystal. The short time interval of the laser flash permits following changes in scattering in time dependent processes, as has been done, for example, during the creep of polyethylene.[7]

Sample-to-film distance is variable to suit the angular range being studied and the photographic film size. For studying scattering at angles less than 5° with 4 x 5" film, a 9" sample-to-film distance proves convenient. With short distances, scattering patterns at up to 30° angle may be recorded. At these large angles, distortion may occur, however, because of incomplete polarization resulting from the acute angle at which the light beam passes through the analyzer. Short distances have the advantage of requiring less exposure time.

PHOTOGRAPHIC METHODS FOR FIBERS

Photographic diffraction patterns obtained by passing a parallel light beam past a fiber of the type shown in Fig. 7 were first described by Thomas Young.[8,9] Up to 20 orders of diffraction may be obtained from a uniform fiber and proves to be a convenient and accurate means for determining fiber diameter.

Raman and Bhat, using polarized light with fibers have described[10] diffraction experiments that depend upon size, surface texture, birefringence and internal heterogeneity. Only a qualitative characterization was possible by this procedure.

By carefully immersing fibers in a medium of matching refractive index it is possible to suppress the scattering and diffraction arising from the fiber surface and obtain patterns which are principally characteristic of the internal structure. For example, Fig. 8 shows the H_V patterns for a parallel bundle of nylon filaments (with the incident light polarized parallel to the fiber axis). The four-leaf clover type of H_V pattern similar to that obtained with films is obtained when the refractive index of the silicone immersion oil is 1.533 which apparently matches that of the fiber. When the refractive index is higher or lower than this, the scattering of the internal structure is obscured by the horizontal streak which arises from the surface contribution.

This principle of eliminating surface scattering by matching the refractive index of the fiber with that of the medium has been utilized in the "fiber refractometer" for the measurement of the refractive indices of fibers.[11,12]

A V_V scattering pattern of an immersed fiber is shown in Fig.9 which again is similar to those obtained from spherulitic films. It is more difficult to suppress the V_V scattering by immersion because the reflected and diffracted light from the surface is preferentially polarized vertically, and the residual horizontal streak results from imperfect matching of refractive index.

Scattering patterns may be obtained from single fibers as well as bundles. In Fig. 10, laser scattering photographs are shown for a single filament, six filaments and a larger bundle. The multifilament bundle shows more diffuseness similar to that obtained with thick film in Fig. 4. With fewer filaments, it is necessary to use more flashes of the laser to obtain sufficient intensity.

INTERPRETATION OF SCATTERING PHOTOGRAPHS

Scattering at these low angles must result from structural heterogeneities larger than the wavelength of light. These heterogeneities may be (a) voids, (b) areas of differing density or crystallinity, (c) areas of differing anisotropy, and (d) anisotropic areas of differing orientation. It is possible to experimentally distinguish among these contributions. Contributions (a) and (b) are referred to as *density fluctuations*. In this case the difference between the refractive indices of these differing areas is larger than the anisotropy of these areas, the scattering pattern will be independent of the direction of polarization of the light, since the difference in induced dipole moment of the two areas is independent of orientation of the polarization direction. This is shown schematically in Fig. 11 for two orientations of polarization. In Figure 12 light

scattering patterns originating from the density fluctuations of the craze cracks in a trifluoroethylene copolymer are shown for two directions of polarization. The small difference proves that the scattering originates primarily from these density heterogeneities. For comparison, scattering patterns for spherulitic polyethylene are shown in Fig. 13 for two directions of polarization. As can be seen, the pattern completely shifts its orientation with a shift in polarization direction. This is a consequence of the pattern arising almost completely from the anisotropy resulting from the difference between the radial and tangential refractive indices of the spherulites.[5] As can be seen in Fig. 14, the orientation of the dipolar distribution depends upon the polarization direction for a spherulite with greater tangential than radial polarizability.

Another means of distinguishing between density and orientation contributions to scattering is through the comparison of V_V and H_V scattering. As can be seen in Fig. 11, the induced dipoles in an isotropic structure with density heterogeneities will be parallel to the polarization direction. The scattered light will be polarized parallel to the dipole direction. Consequently, if this is analyzed with a horizontally oriented polaroid (as with H_V scattering), no light will be transmitted. For anisotropy or orientation fluctuation type contributions, however, this is not true. It is apparent from Fig. 14 and the theory presented elsewhere[5,13] that, because the polarizability is a tensor quantity in this case, the induced dipoles are not necessarily parallel to the polarization direction and a resulting component of scattered radiation will be transmitted through a horizontal analyzer.

To illustrate, in Fig. 15, the V_V and H_V scattering photographs are shown for a partly crystallized polyethylene sample in which the principal

contribution is from the density difference between the partly crystalline spherulites and their amorphous surroundings. The absence of a pronounced H_v pattern is evidence of the density fluctuation origin. This may be compared with Fig. 2 for a completely spherulitic sample where the comparable intensities of the H_v and V_v patterns prove that orientation fluctuations are the principal contributor.

A fourth method for distinguishing between density and orientation contributions involves the use of a liquid which will imbibe one of the phases and change the average refractive index difference causing density fluctuation scattering. Thus, if this scattering arises from the refractive index difference between *vacuo* within voids and the surrounding polymer, a solvent which enters the voids will greatly decrease this refractive index difference and diminish the scattering. Similarly, if scattering results from the refractive index difference between the amorphous and crystalline regions of a polymer, a liquid which will swell the amorphous regions but not the crystalline regions should greatly affect this difference and change the scattering. Since the refractive index difference between these regions is quite small (of the order of 0.03), and the intensity of scattering depends upon the square of this difference, the scattering should be quite dependent upon the refractive index of the swelling liquid and should pass through a minimum when the refractice index of the swollen amorphous phase matches that of the crystallite. In fact, by examining the variation of scattering with the refractive index of the swelling liquid and by measuring the degree of swelling, it is possible to estimate the refractive index difference originally causing the scattering.

To illustrate this approach, Fig. 16 shows the V_v scattering pattern of a crazed polycarbonate film without and with imbibing acetone which greatly decreases the intensity of the V_v scattering arising from the density

fluctuation of the craze cracks. On the other hand, the fact that the scattering pattern from a portion of a polyethylene oxide spherulite in Fig. 17 is virtually unaffected by swelling by carbon tetrachloride indicates the orientation variation origin.

SIZE AND SHAPE

The larger the structure, the more rapidly will the scattered intensity decrease with increasing angle between the transmitted and the scattered ray. Consequently, the larger the scattering object, the smaller the scattering pattern. For an unoriented isotropic system, the average size of the scattering object will be the same in all directions and the scattering pattern will have circular symmetry as in Fig. 15. However, for a system which is itself oriented, or for one in which the dipolar distribution is oriented (as in Fig. 14) because of anisotropic scatterers in polarized light, the scattering pattern will be oriented having its greatest dimension along the direction of minimum extension of the scattering object as in Fig. 13.

In the absence of orientation it is not possible to determine simultaneously the size, shape and anisotropy. However, by utilization of other information about the scattering system, one may often assume a model for the shape of the scattering region and determine the size and anisotropy from the scattering pattern. For example, it is known from light or electron microscope studies that spherulitic polyethylene consists of spherical aggregates of crystals with principal refractive indices in the radial and tangential directions. From the theory of scattering from such anisotropic spheres[5,13] the V_V and H_V patterns of Fig. 18 may be calculated which may be compared with the measured patterns of Fig. 2. The distance from the center of the pattern to one of the lobes of the H_V four-leaf clover

depends upon the spherulite size. The scattering angle θ_m corresponding to one of these maxima is given by

$$\frac{4 \pi R}{\lambda} \sin (\theta_m/2) = 4.0$$

where R is the spherulite radius and λ the wavelength of light in the scattering medium. A qualitative indication of this dependence is seen for the H_v scattering patterns for three spherulite sizes in Fig. 19. The spherulite radius calculated in this way has been found to be in good agreement with microscopically measured values both for films and fibers.

ANISOTROPY AND ORIENTATION OF PRINCIPAL AXES

The appearance of the pattern, particularly for the V_v case, is dependent upon the relative values of the radial and tangential refractive index of the spherulite and of the surroundings. For example, Fig. 20 shows a calculated[13] V_v pattern corresponding to the same size spherulite but a different set of polarizabilities from those used for Fig. 18. Some results illustrating this effect are seen in Fig. 21 for V_v patterns for two nylon samples crystallized at different temperatures. The birefringence of the nylon spherulite depends upon its growth temperature. The growth of disc-like rather than spherical spherulites in thin films also predominantly effects the V_v scattering pattern.[13]

The relative orientation of the principal polarizability axes and the direction of maximum extension of the scattering object may be determined from the orientation of the scattering pattern relative to that of the polarization direction. For an unoriented system, if the direction of maximum polarizability is along the direction of maximum extension, the object will scatter most when it is oriented with its long axis parallel to the polarization direction. This will give a V_v scattering pattern oriented

perpendicularly to the stretching direction. The H_v pattern will be most intense when the greatest polarizability direction is at 45° to polarization, which results in a "four-leaf clover" type pattern.[14] A sphere with its maximum polarizability direction in the radial direction is qualitatively optically equivalent to a randomly oriented collection of such rods.

If the direction of maximum polarizability is oriented at an angle, α, to the direction of maximum extension, the V_v scattering pattern maxima will be oriented at an angle $(90° \pm \alpha)$ to the polarization direction and the H_v pattern at $\pm (45° \pm \alpha)$.

Thus, the pattern arising from the internal structure of Teflon shown in Fig. 3(b) in which the V_v maxima are oriented at 45° to polarization indicates that α=45° for this material. One would predict, in agreement with observation,[14] that the H_v maxima should occur at 0° and 90° to polarization. This would mean that Teflon can be considered as a disoriented collection of rod-like structures in which the principal polarizability direction is at 45° to the rod axis, or else to contain spherulites with their principal polarizability axes at 45° to the radius. The former interpretation is in better agreement with the observed morphology[14] for the samples studied.

ORIENTATION OF SAMPLES

The orientation of scattering superstructure within a sample may be determined from the rotation of the scattering pattern occurring when the film sample is rotated about its normal (coincident with the incident light beam). Thus, in Fig. 12, the orientation of the density fluctuation pattern is determined by the orientation of the craze cracks (normal to the stretching direction of the polychlorotrifluoroethylene) and would rotate if the sample is rotated. In the case of stretched polyethylene where there are

perpendicularly to the stretching direction. The H_v pattern will be most intense when the greatest polarizability direction is at 45° to polarization, which results in a "four-leaf clover" type pattern.[14] A sphere with its maximum polarizability direction in the radial direction is qualitatively optically equivalent to a randomly oriented collection of such rods.

If the direction of maximum polarizability is oriented at an angle, α, to the direction of maximum extension, the V_v scattering pattern maxima will be oriented at an angle $(90° \pm \alpha)$ to the polarization direction and the H_v pattern at $\pm (45° \pm \alpha)$.

Thus, the pattern arising from the internal structure of Teflon shown in Fig. 3(b) in which the V_v maxima are oriented at 45° to polarization indicates that α=45° for this material. One would predict, in agreement with observation,[14] that the H_v maxima should occur at 0° and 90° to polarization. This would mean that Teflon can be considered as a disoriented collection of rod-like structures in which the principal polarizability direction is at 45° to the rod axis, or else to contain spherulites with their principal polarizability axes at 45° to the radius. The former interpretation is in better agreement with the observed morphology[14] for the samples studied.

ORIENTATION OF SAMPLES

The orientation of scattering superstructure within a sample may be determined from the rotation of the scattering pattern occurring when the film sample is rotated about its normal (coincident with the incident light beam). Thus, in Fig. 12, the orientation of the density fluctuation pattern is determined by the orientation of the craze cracks (normal to the stretching direction of the polychlorotrifluoroethylene) and would rotate if the sample is rotated. In the case of stretched polyethylene where there are

oriented fluctuations, the pattern depends upon the orientation of both the sample and the polarizers. For example, in Fig. 23 rotating the sample produces changes in the orientation, intensity and nature of the V_V pattern.

For unoriented polymers, the H_V pattern has four fold symmetry about the perpendicular directions of the polarizer and analyzer (Figs. 2 and 22). For a stretched polymer (stretching along one of the polarization directions) the pattern has only two fold symmetry along the stretching direction. (Fig. 24). In both cases (which are typical) the pattern becomes elongated perpendicular to the stretching direction and decreases in intensity upon stretching. The former effect is a consequence of the usual tendency for a structure to align itself with its long dimension parallel to the stretching direction of the sample. The intensity decrease results from the alignment of the principal polarizability direction parallel to the stretching direction. Then the induced dipoles become parallel to the polarizer and little scattered light is transmitted through a perpendicular analyzer.

Since in Teflon the principal polarizability direction is initially at about 45° to the direction of maximum extension, the above observation indicates that stretching is accompanied by a rotation of the principal polarizability axis within the scattering entity. Thus, stretching does not only involve the orientation of the crystalline aggregate but also a rearrangement of crystals within the aggregate.

Similar conclusions have been reached concerning the deformation of polyolefins[5,15,16,17,18,19] where elongation is postulated to be a two stage process; first involving the reversable affine deformation of the spherulitic structure, followed by the reorientation of the crystals within this structure. Quantitative interpretation of the accompanying light

scattering pattern changes is dependent upon the claculation of the scattering patterns of deformed spherulites.

SCATTERING RESULTING FROM STRAINS SURROUNDING HETEROGENEITIES

In some cases, orientation fluctuation type patterns characteristic of structure several microns in size arise upon stretching a polymer. Crystallization does not occur upon stretching in those cases and there is no evidence for the formation of spherulitic structures. Microscopic examination reveals the presence of voids in some of these samples which become deformed to ellipsoids upon stretching (Fig. 25). The polymer surrounding these deformed voids exhibit birefringence patterns between crossed polaroids.

Thus, these regions surrounding deformed voids are optically anisotropic and act as scattering centers. In the unstretched state the strain pattern surrounding such voids has its principal polarizability axes in the radial and tangential directions, and the situation is similar to that described by Goldstein[20,21] for strains surrounding defects in glasses. Upon deforming however, the strain becomes greater and the direction of the principal axes changes. This would give rise to a deformed H_v four-leaf clover type of pattern of size characteristic of that of the strain region (Fig. 26). The strain pattern also contributes to the V_v pattern with greater elongation of the pattern perpendicular to the stretching direction (Fig. 26). The density fluctuation of the void, itself, also contributes to V_v (but not H_v) and this is superposed upon the V_v strain pattern. Hence, the V_v pattern is considerably more intense than the H_v. It follows (as has been observed), that imbibing a liquid which fills the voids but does not swell the polymer depresses the density fluctuation contribution but not the strain contribution. The strain pattern may be

depressed, however, by relaxation with a swelling solvent or by heating above the glass temperature.

Strain patterns may also arise about growing crystallites as well as about voids as a consequence of the strains imposed upon the surrounding amorphous polymers. Thus, the increase in turbidity accompanying the crystallization of a polymer may arise from several causes including (a) the refractive index difference between the crystals and the amorphous surroundings, (b) the refractive index difference between the partly crystalline growing spherulites and their amorphous surroundings, (c) the orientation fluctuations resulting from correlated orientation within crystalline superstructure, (d) strain produced anisotropy in the amorphous surroundings of growing crystals or spherulites, and (e) void formation arising from dilational strains accompanying the density change which occurs during crystallization. The various contributions may be resolved by employing the preceding techniques, by making simultaneous studies by other techniques, or by additional experiments. For example, the turbidity accompanying void formation during crystallization may often be reduced by closing the voids by rubbing the sample with a hard object or by rolling.

INTERNAL STRUCTURE

The preceding discussion of scattering from spherulites and other aggregates reflected contributions from internal heterogeneities. It has been shown,[22] subject to certain approximations, that the total scattering from a heterogeneous sphere, for example, is the sum of the contribution from an equivalent homogeneous sphere plus that of the heterogeneities. A case considered in detail[23] is that of a spherulite with radial periodicity

of orientation of the optic axes. In the V_V scattering pattern from such spherulites (Fig. 27) a scattering maximum at wider angles (around 15°) occurs characteristic of this periodicity.[24,25] The intensity of these maxima is much less than that of the low angle maximum and exposure times of several hours are required. The orientation of this maximum with respect to the polarization direction proves the orientation origin of this periodicity.

The scattering at still greater angles is greater than that expected for uniform spheres. This is a result of shorter range correlation of orientation of crystals within the spherulite. The intensity contribution at these large angles is too low to study in a practical manner by the photographic technique.

HETEROGENEITY OF STRUCTURE

In most cases, the incident light beam has a diameter considerably greater than that of the spherulite or structural heterogeneities. The scattering pattern, in these cases, is an average over that of all of the structure within the beam. If there is no correlation among neighboring heterogeneities, the scattered intensity is the sum of that from the individual heterogeneities. The effect of a distribution of sizes of spherulites upon the broadening of the scattering pattern has been analyzed according to this principle.[26]

If two types of structure are present simultaneously, the scattering pattern will be a sum of that from both types of structure. For example, for annealed stretched polyethylene, the H_V pattern of Fig. 28 is a sum of two patterns, one originating from the partially disoriented, stretched structure, and the other from a new structure produced by recrystallization

accompanying annealing.[15]

PHOTOMETRIC STUDIES

Methods for measuring the scattering from polymer films by a photomultiplier photometer have been described and reviewed.[1,2,3,27,28] Recent developments in technique include the use of a computer program for applying correction factors and for data reduction.[29] Current interpretations have utilized an extension of the theory of Goldstein and Michalik[30] by Stein and Wilson[31] for scattering at wide angles resulting from short range correlation of crystal orientation. The Debye-Bueche exponential correlation function[32] which is found experimentally has recently been justified in terms of a "random walk" theory of correlated crystal orientation.[33] Experimental methods and interpretations proposed for oriented systems[18] have been extended for biaxial orientation by Hotta and Stein.[34]

Photometric techniques for studies of fibers have recently been described[35] and interpretations in terms of cylindrically symmetrical type correlation function have been proposed.[35,36] Results on polycaprolactam fibers are presented.

ACKNOWLEDGMENT

The authors are indebted to Monsanto Chemical Company, E.I.duPont deNemours and Company, General Electric Company, Chemstrand Research Center, and Allied Chemical Company for samples used in these studies. They are also indebted to Dr. S.Chatterjee and Mr. George Adams for use of unpublished results.

REFERENCES

1. R.S.Stein, J.J.Keane, F.H.Norris, F.A. Bettelheim and P.R. Wilson, Ann.New York Acad. Sci., 83, 37 (1959)

2. R.S.Stein, M.B. Rhodes, P.R. Wilson and S.N. Stidham, Pure and Applied Chemistry. Vol.IV, Butterworth, London (1962), p.219

3. R.S. Stein, Proceedings of the Interdisciplinary Conference on Electromagnetic Scattering, (Potsdam, N.Y., June, 1962) Pergammon Press, in press.

4. A. Plaza, F.H. Norris, and R.S.Stein, J. Polymer Sci., 24, 455 (1957)

5. R.S. Stein and M.B. Rhodes, J. Appl. Phys., 31 , 1873 (1960)

6. M.B. Rhodes, D.A. Keedy, and R.S. Stein, J. Polymer Sci., 62, S73 (1962)

7. R.S. Moore, Bell Telephone Labs., private communication.

8. T. Young, Encyclopedia Brittanica, 4th and 6th Ed. (1824)

9. R. Meredith and J.W.S. Hearle, Physical Methods of Identifying Textile Fibers, Textile Book Publishers (Interscience), New York (1959), p.164

10. C.V. Raman and M.R. Bhat, Proc.Indian Acad.Sci., A40, 109 (1954)

11. J.M. Preston and R.V. Bhat, J. Text. Inst., 39, T211 (1948)

12. K. Freeman and J.M. Preston, J.Text.Inst., 34, T19 (1943)

13. R.S. Stein and P.R. Wilson, ONR Technical Report No. 35, Project NR 356-378 Contract Nonr 3357 (00), Dept. of Chemistry, Univ. of Mass., Amherst, Mass., Aug. 25, 1961.

14. M.B. Rhodes and R. S. Stein, J. Polymer Sci., 62, S84 (1962)

15. M.B. Rhodes and R.S. Stein, J. Appl. Phys., 32, 2344 (1961)

16. S. Hoshino, J. Powers, D.G. LeGrand, H.Kawai and R.S.Stein, J. Polymer Sci., 58, 185 (1962)

17. R.S. Stein and F.H. Norris, J. Polymer Sci., 21, 381 (1956)

18. F.H. Norris and R.S. Stein, J.Polymer Sci., 27, 87 (1958)

19. K. Sasaguri,S. Hoshino and R.S. Stein , papers to be presented at American Phys. Soc. Mtg., St.Louis, Missouri , March 1963 and the American Chem. Soc. Mtg., Los Angeles, California, April, 1963.

Ref. - cont.

20. M.Goldstein, J. Appl.Phys., 30, 501 (1959)

21. M. Goldstein, Ford Motor Company Scientific Laboratory Report, April 30, 1962.

22. R.S.Stein, P.R.Wilson, and S.N. Stidham, J.Appl.Phys., 34,46 (1962)

23. R.S.Stein, ONR Technical Report No. 9, Contract Nonr 2151(00), Project NR 356-378, Dept. of Chemistry,Univ.of Mass.,February 10,1959

24. R.S. Stein and A.Plaza, J.Polymer Sci., 45, 519 (1960)

26. R.S. Stein, S.N. Stidham and P.R. Wilson, ONR Technical Report No. 26 Project 356-378, Contract 3357(00),Univ. of Mass., Amherst, Mass., August 10, 1961.

27. R.S. Stein and J.J. Keane, J.Polymer Sci., 17, 21 (1955)

28. J.J. Keane and R.S. Stein, J. Polymer Sci., 20, 327 (1956)

29. R.S. Stein, S.N. Stidham and P.R. Wilson, ONR Technical Report No. 34 Project 356-378, Contract Nonr 3357(00), Univ. of Mass., Amherst, Mass., July 10, 1961.

30. M. Goldstein and E.R. Michalik, J. Appl. Phys., 26, 1450 (1955)

31. R.S. Stein and P.R. Wilson, J. Appl.Phys., 33, 1914 (1962)

32. P. Debye and A. Bueche, J. Appl. Phys., 20 518 (1949)

33. R.S. Stein, unpublished work

34. T. Hotta and R.S. Stein, unpublished work

35. Ch.Ruscher and J. Dechant,Faserforschung and Textiltechnik 13, 166, 203 (1962)

36. Ch. Ruscher and J. Dechant, Monats.Deutch.Akad. Wissenschaten Berlin 4, 393 (1962)

CAPTIONS FOR FIGURES

1. The photographic low-angle scattering apparatus.

2. Typical V_V and H_V scattering patterns of medium density polyethylene.

3. Light scattering photographs from a Teflon film (a) poor refractive index match immersion fluid n = 1.50 (b) good refractive index match n = 1.38.

4. The effect of film thickness on scattering patterns from a medium density polyethylene film (a) 3 mil film, (b) 10 mil film.

5. Stray reflections arising from poor alignment of optical surfaces.

6. The arrangement for photographic light scattering using a laser source.

7. The diffraction pattern from a nylon monofilament.

8. The effect of refractive index of a silicone oil immersion fluid on the H_V scattering pattern for a parallel bundle of nylon filaments.

9. A V_V scattering pattern for an immersed parallel bundle of fibers.

10. H_V scattering patterns for (a) a bundle of nylon filaments, (b) six filaments, and (c) a single filament.

11. The distribution of dipoles in a structure with density differences in vertically and horizontally polarized light.

12. V_V scattering patterns for crazed oriented polytrifluoroethylene copolymer for two directions of polarization.

13. V_V scattering patterns from unstretched spherulitic polyethylene for two directions of polarization.

14. The distribution of dipoles in anisotropic spherulites for two directions of polarization.

15. V_V and H_V scattering photographs for a partially spherulitic polyethylene sample illustrating the consequence of a density fluctuation origin of scattering.

16. V_V scattering patterns of a crazed polycarbonate film without and with the presence of imbibing acetone (a) without (b) with.

Figures - cont.

17. V_V scattering patterns of a portion of a polyethylene oxide spherulite without and with swelling carbon tetrachloride (about 15%) (a) without (b) with.

18. Calculated V_V and H_V scattering patterns from an anisotropic sphere.

19. H_V scattering patterns for three sizes of polyethylene spherulites. Diameters are (a) 2.0μ (b) 3.5μ and (c) 8.7μ.

20. A calculated V_V scattering pattern for a different set of polarizabilities than that used in Fig. (18).

21. V_V scattering patterns from spherulitic Nylon 66 crystallized at two temperatures.

22. An H_V scattering pattern from the internal structure of unstretched Teflon.

23. The change in V_V scattering pattern produced by rotating a stretched polyethylene film (a) stretched vertically and (b) horizontally.

24. H_V scattering patterns for vertically stretched samples of (a) polyethylene and (b) Teflon.

25. Deformed voids in a stretched polycarbonate sample.

26. V_V and H_V patterns arising from the strain pattern surrounding deformed voids in a stretched polycarbonate film.

27. The V_V scattering pattern from a spherulite having radial periodicity of crystal orientation, leading to a "ringed" appearance.

28. An H_V scattering pattern from annealed, stretched polyethylene.

FIG 1

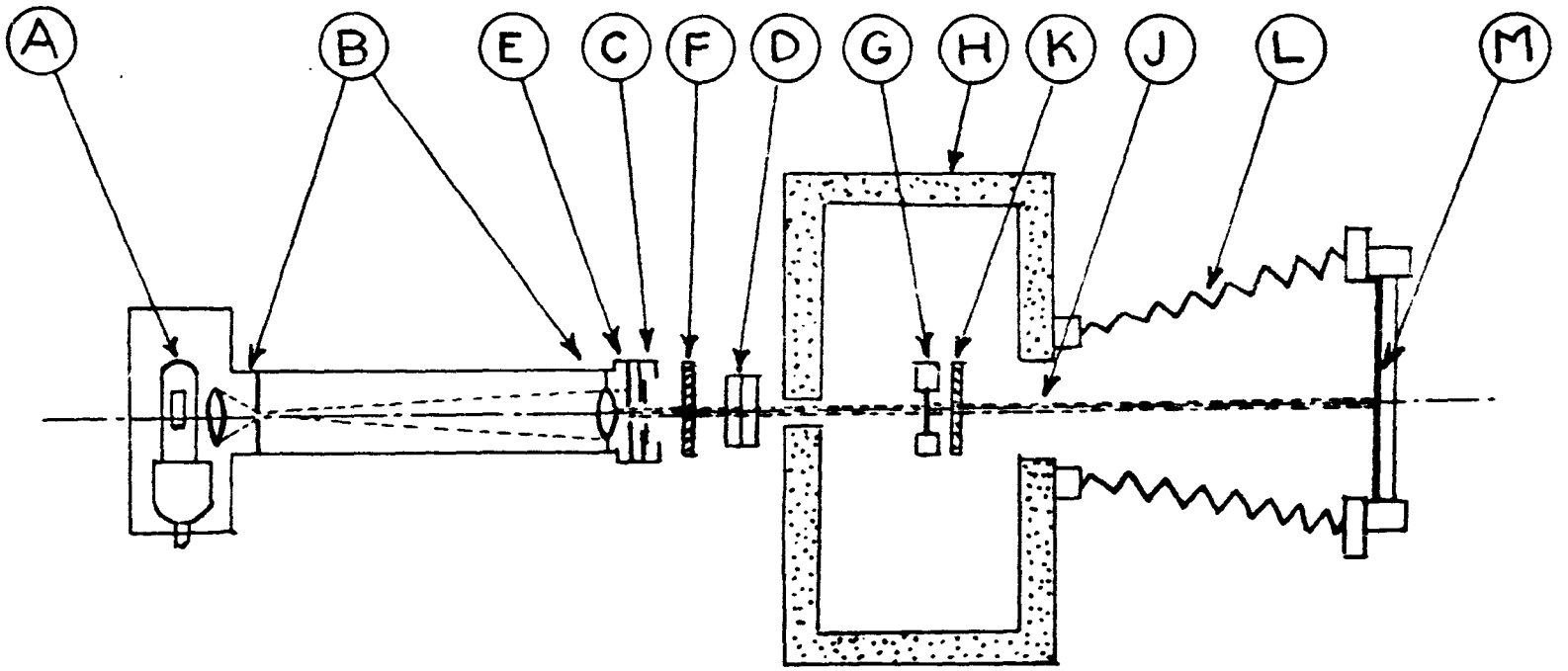

Fig. 1. The photographic low-angle scattering apparatus. (A) Light source. (B) Lens and pinhole system. (C) Shutter. (D) Filters. (E) Iris diaphragm. (F) Polarizer. (G) Sample. (H) Constant temperature chamber. (J) Exit window. (K) Analyzer. (L) Bellows. (M) Film holder.

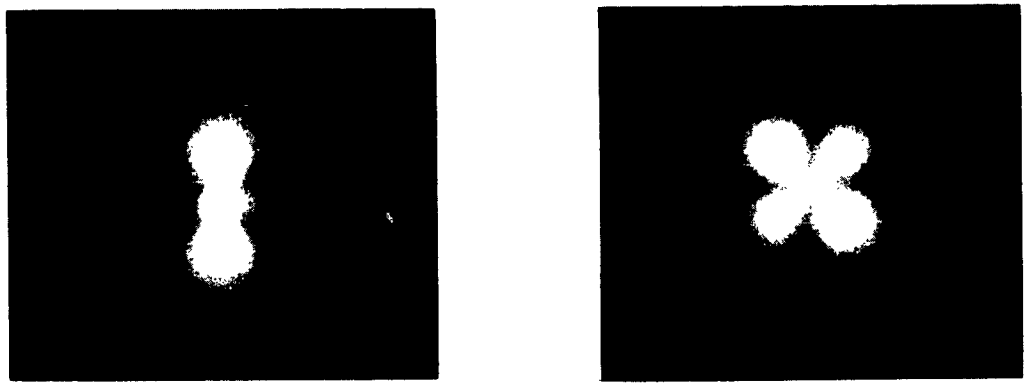

Fig. 2

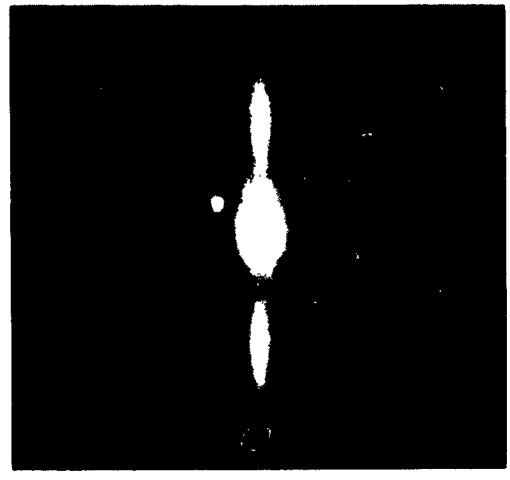

(a)

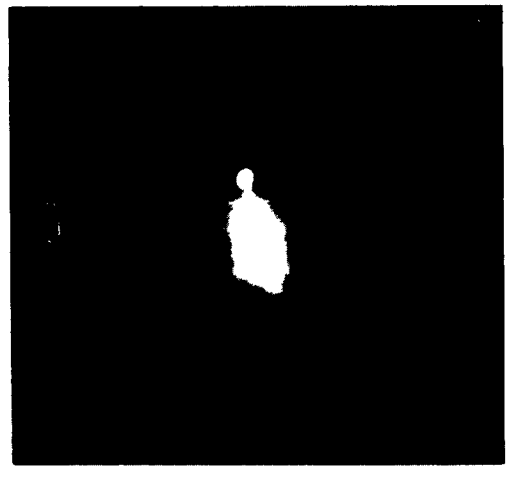

(b)

Fig. 3

(a) (b)

Fig. 4

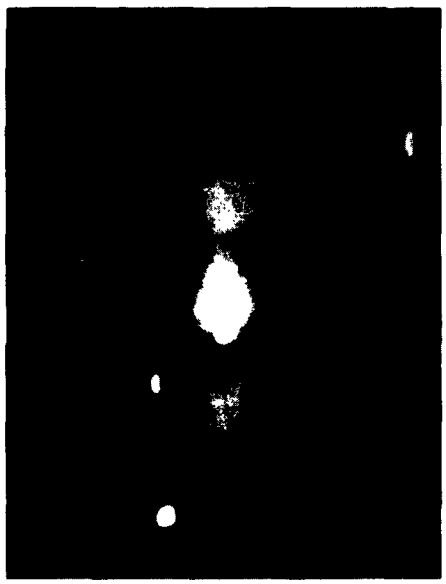

Fig. 5

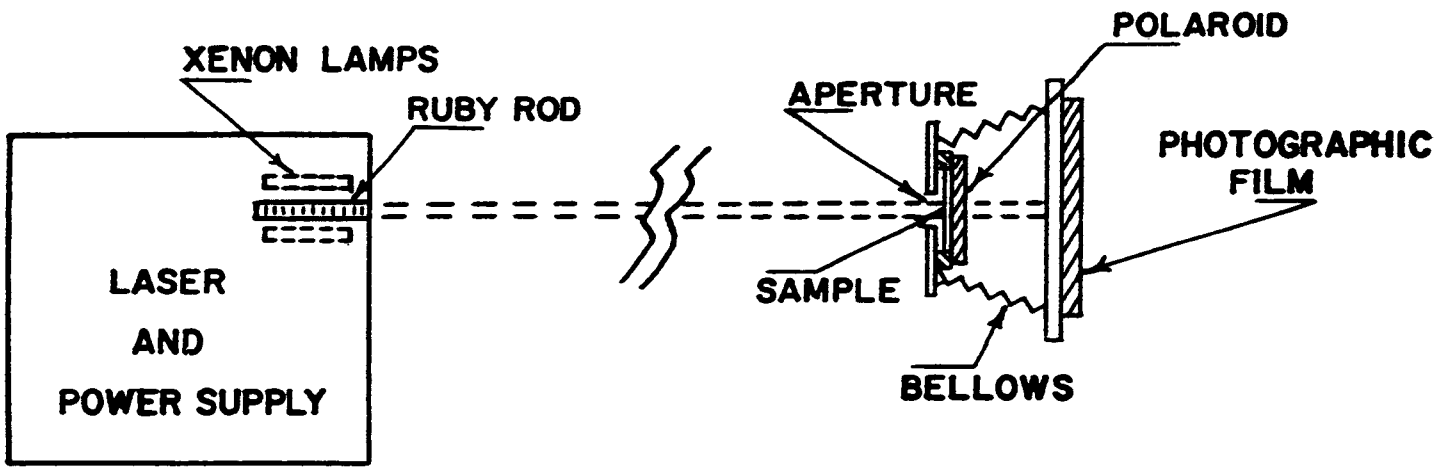
XENON LAMPS
RUBY ROD
LASER
AND
POWER SUPPLY
APERTURE
POLAROID
PHOTOGRAPHIC
FILM
SAMPLE
BELLOWS

Fig 6

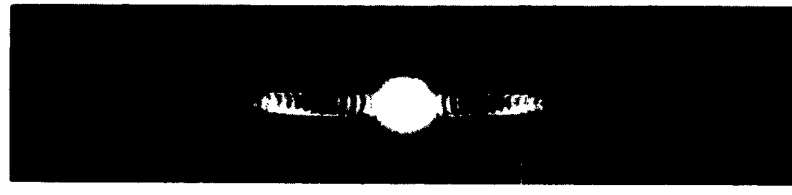

Fig. 7

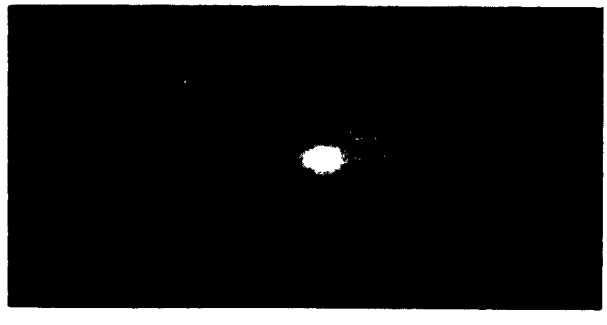

n=1.402

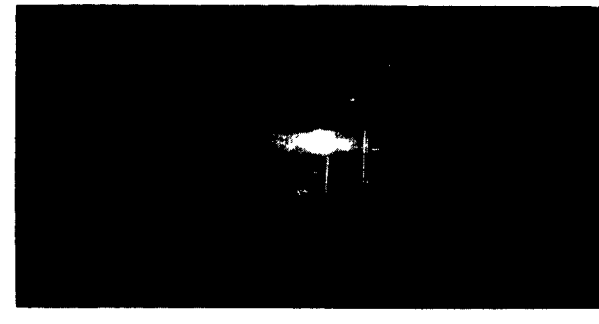

n=1.575

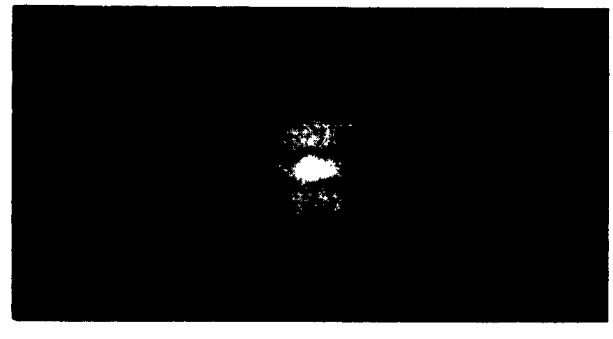

n=1.537

Fig. 8

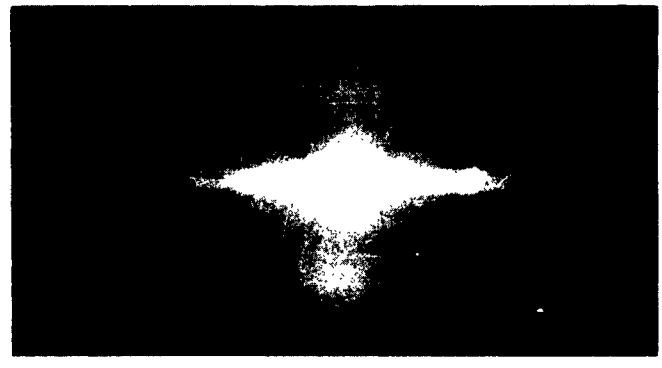

Fig. 9

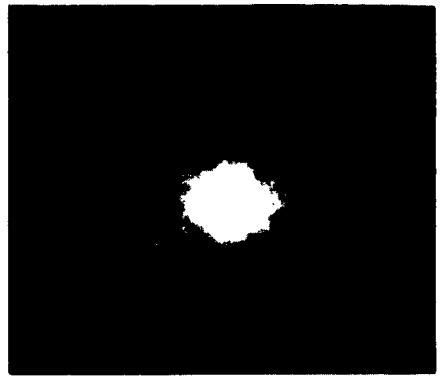

(a)

(b)

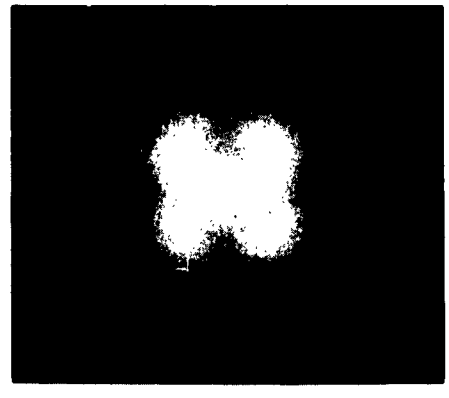

(c)

Fig. 10

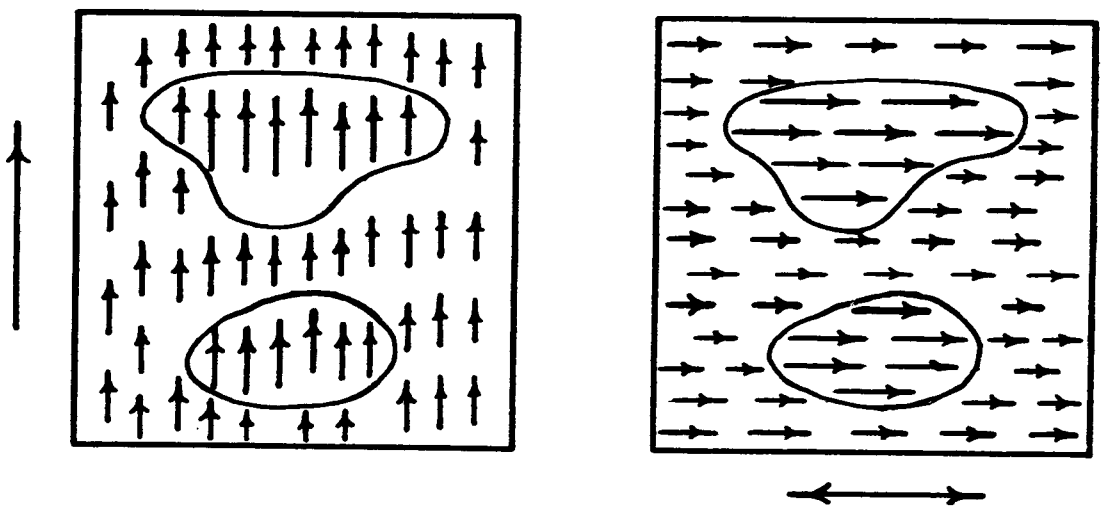

Fig. 11

HH

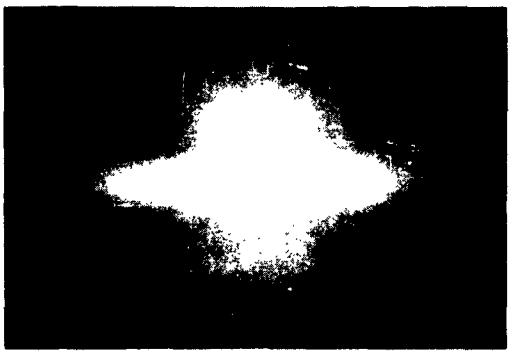

Vv

STRETCH DIRECTION ⟶

Fig. 12

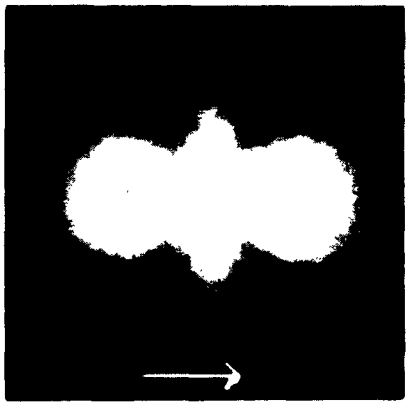

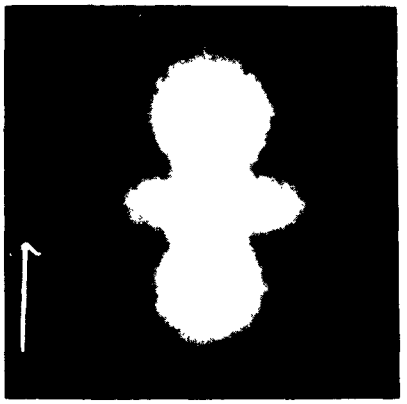

Fig. 13

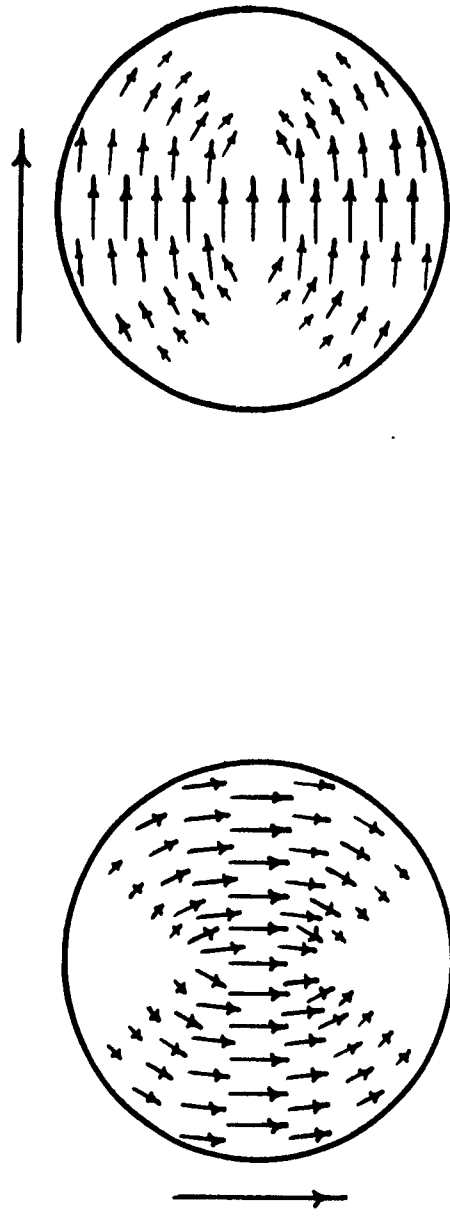

Fig. 14

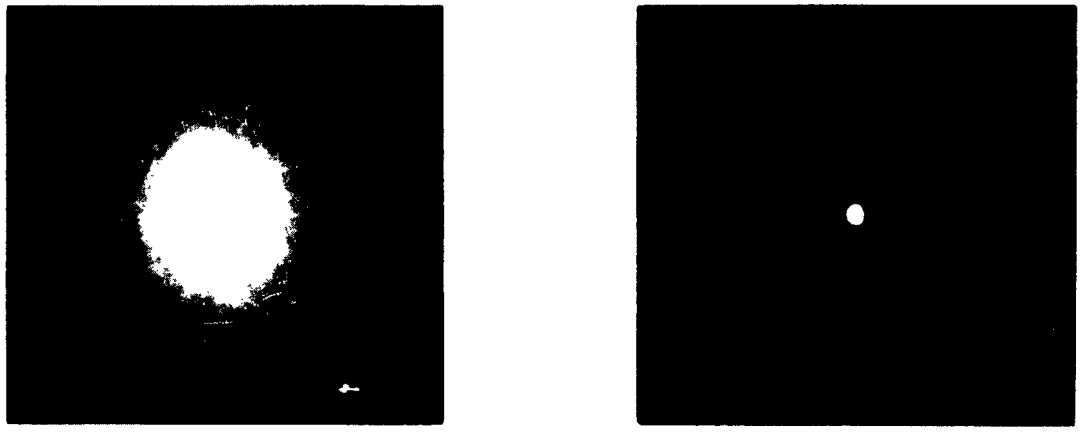

Vv Hv

Fig. 15

(a) (b)

Fig. 16

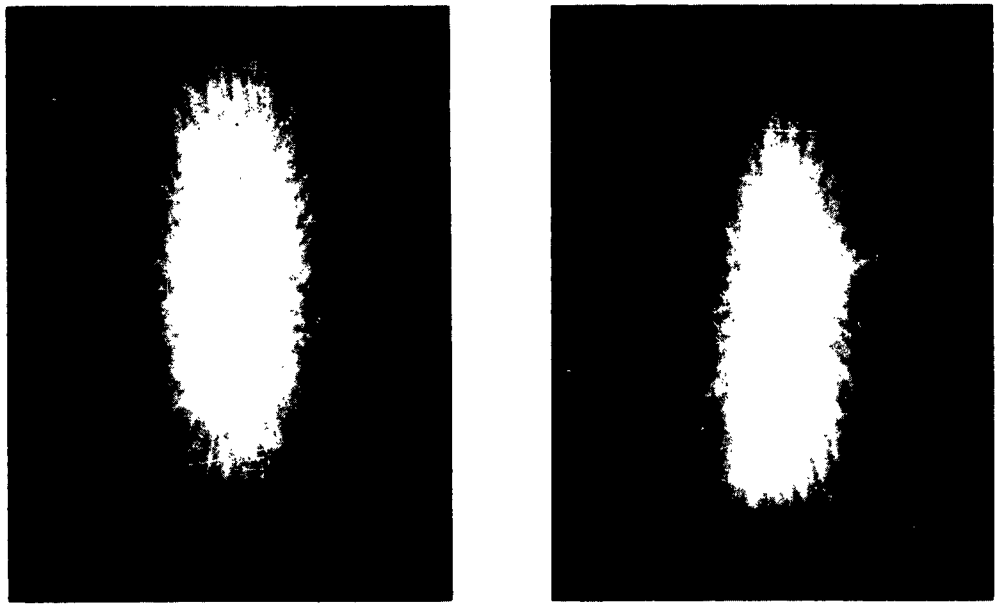

(a) (b)

Fig. 17

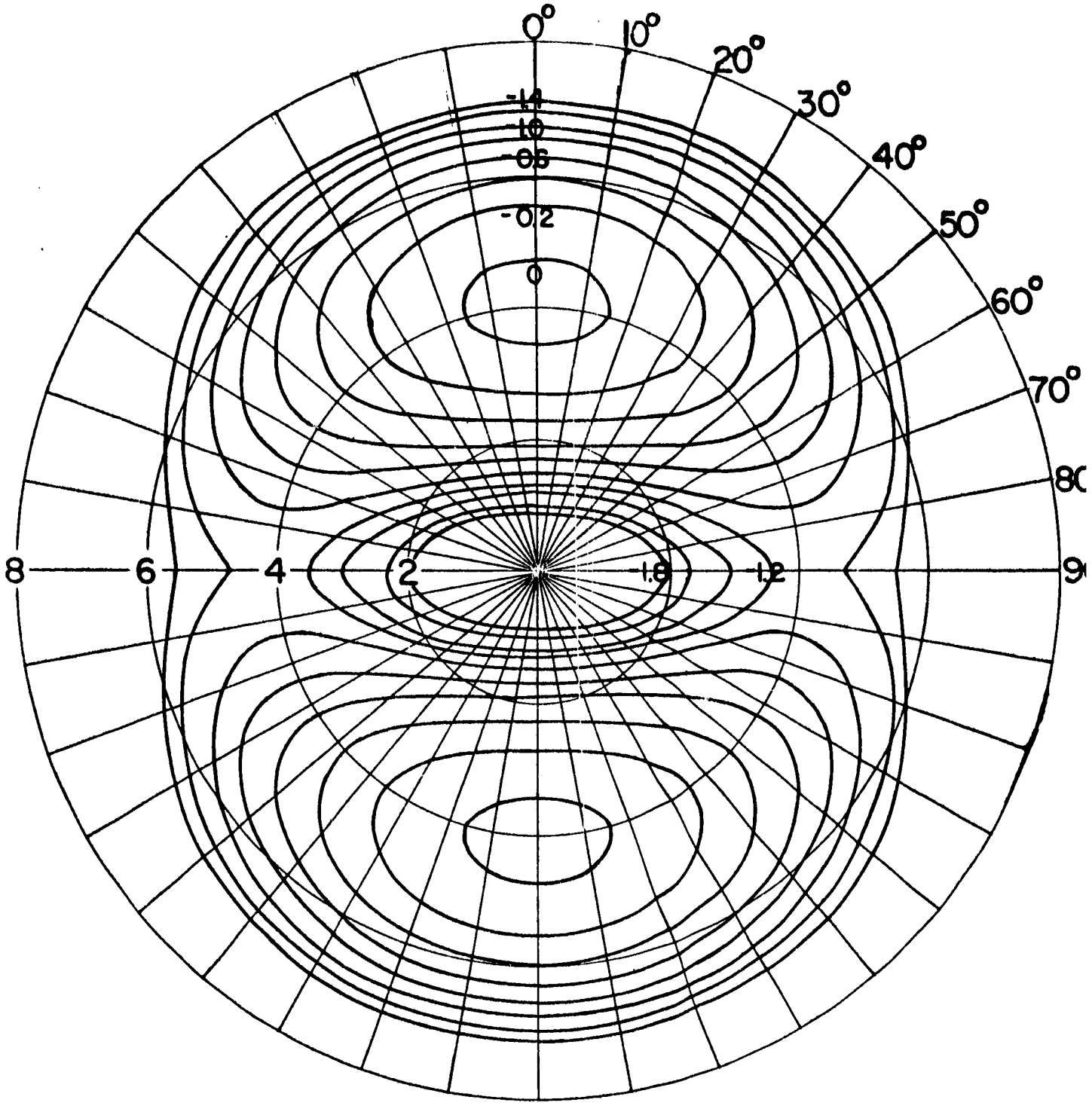

FIG. 18 V_v

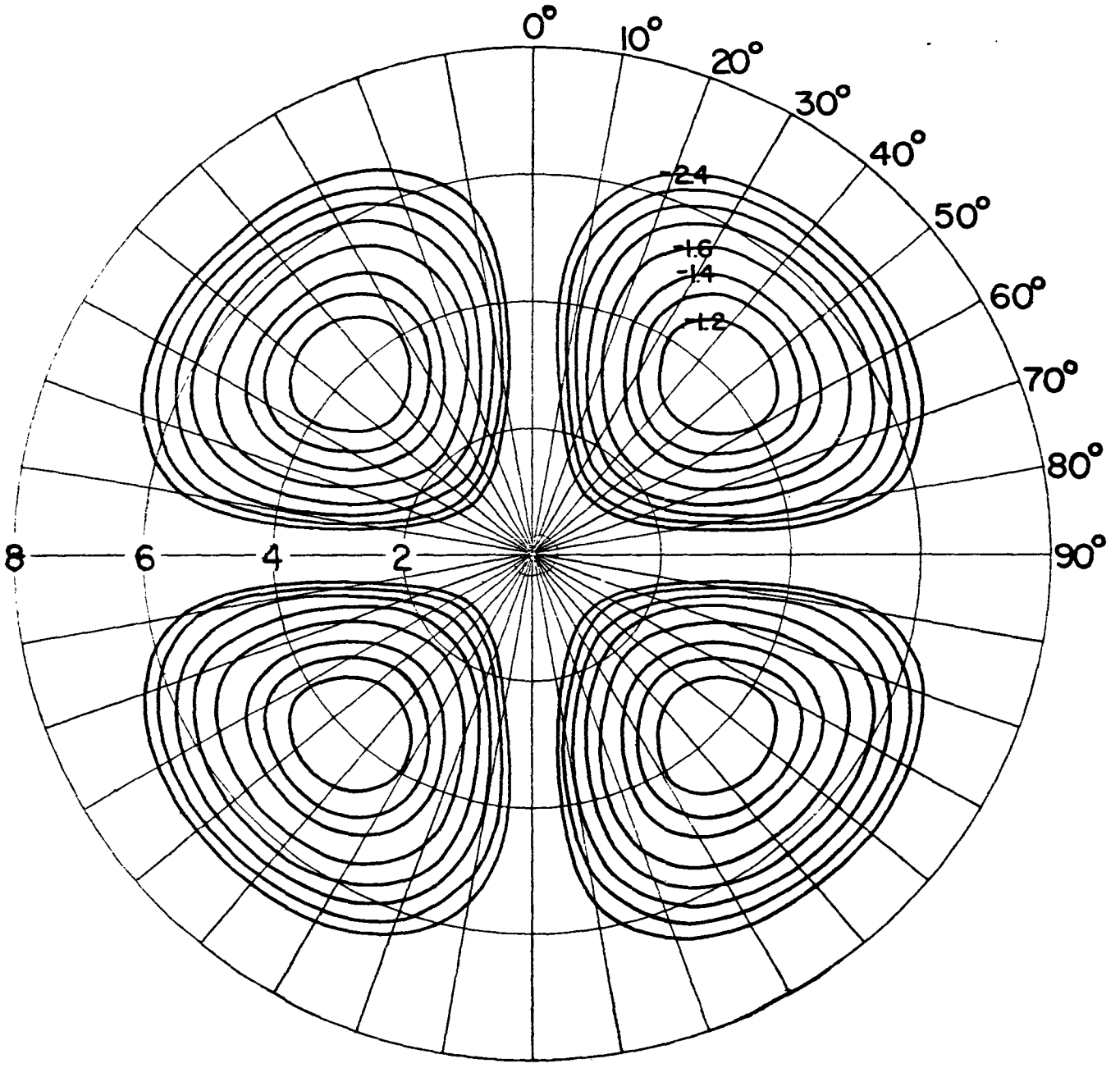

FIG. 18 E_V

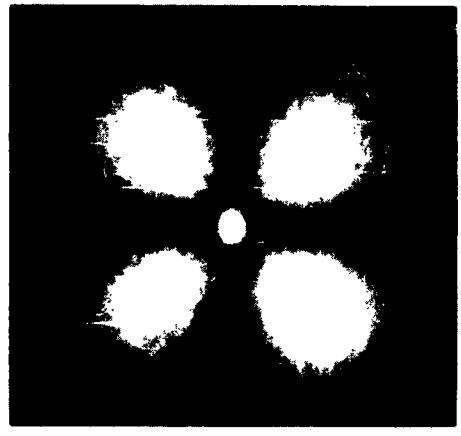

(a)

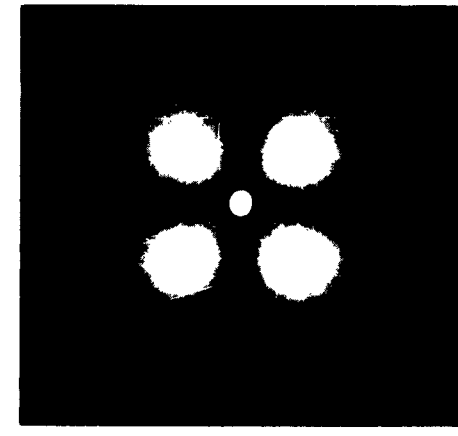

(b)

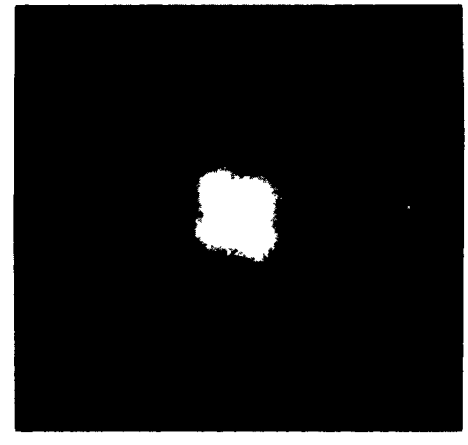

(c)

Fig. 19

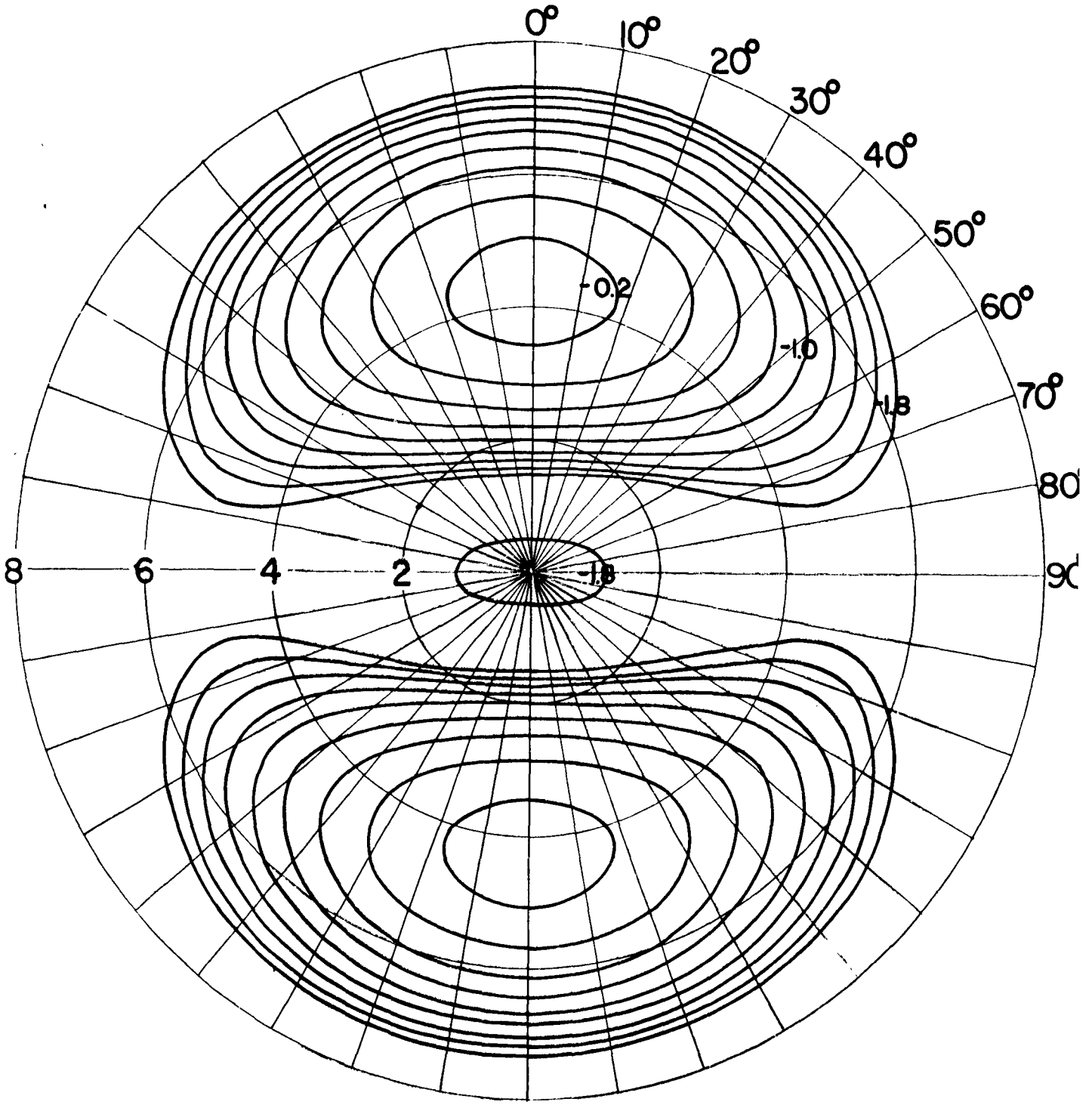

FIG. 20

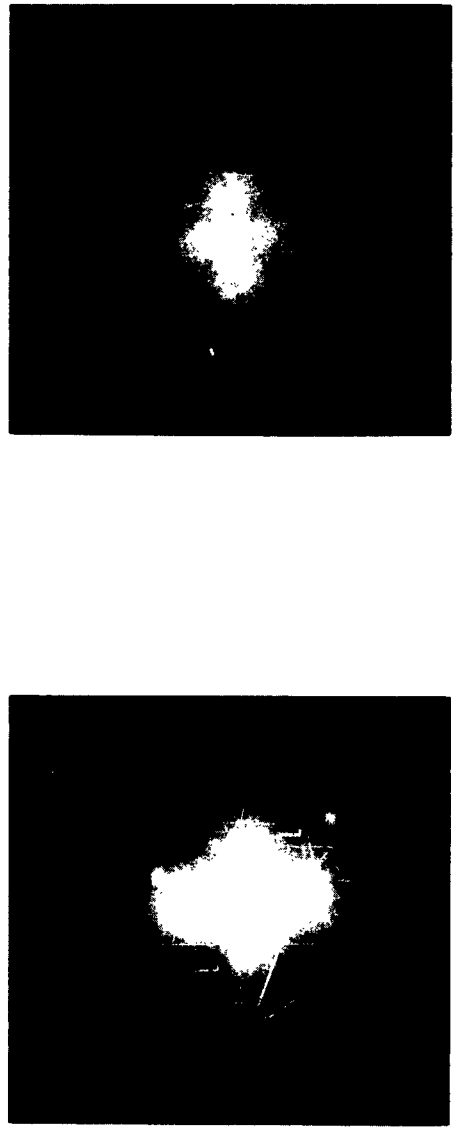

Fig.21

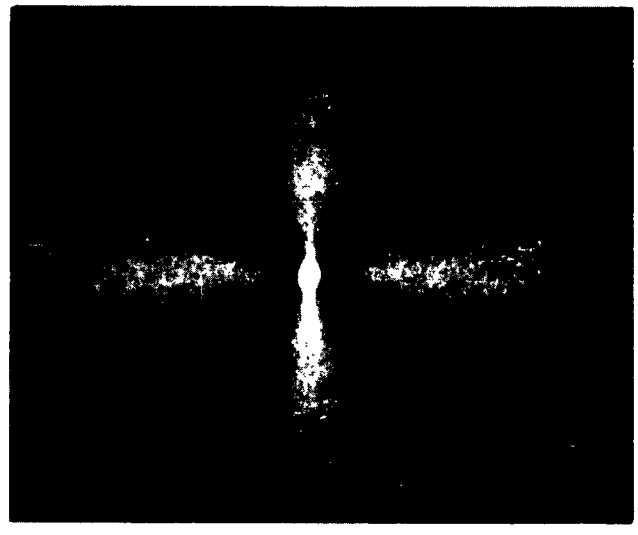

Fig. 22

(a) (b)

Fig. 23

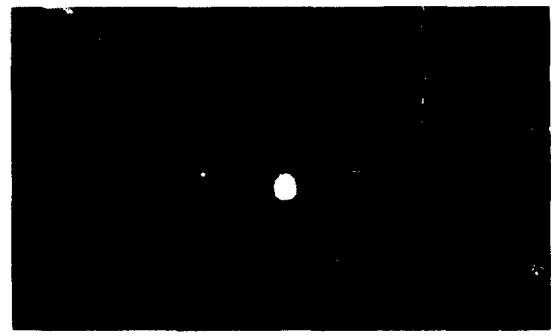

(a)

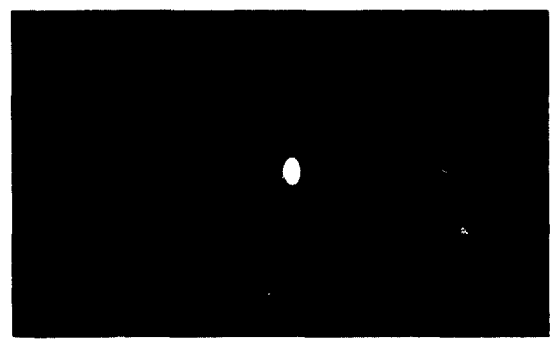

(b)

Fig. 24

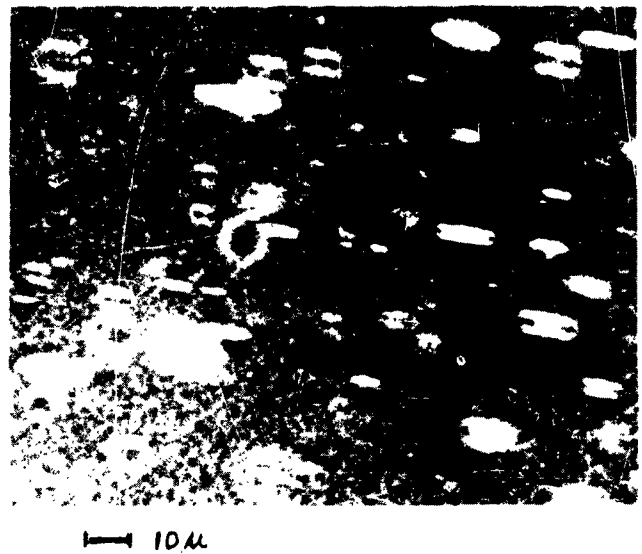

Fig.25

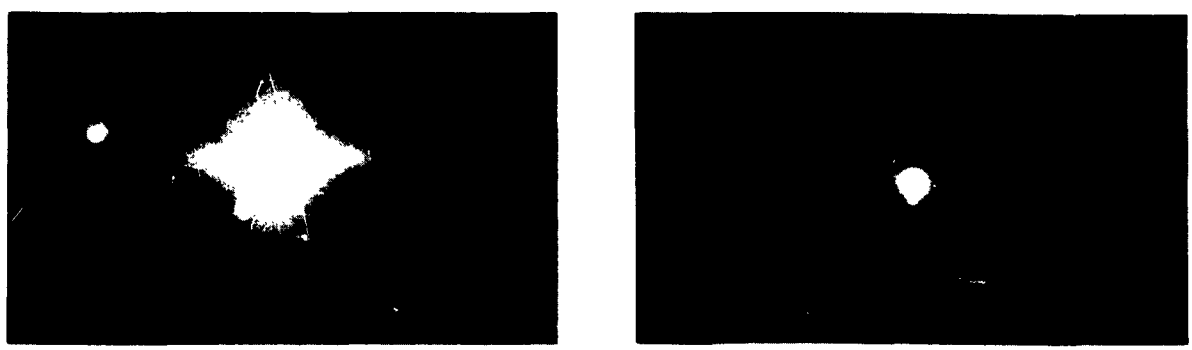

Fig.26

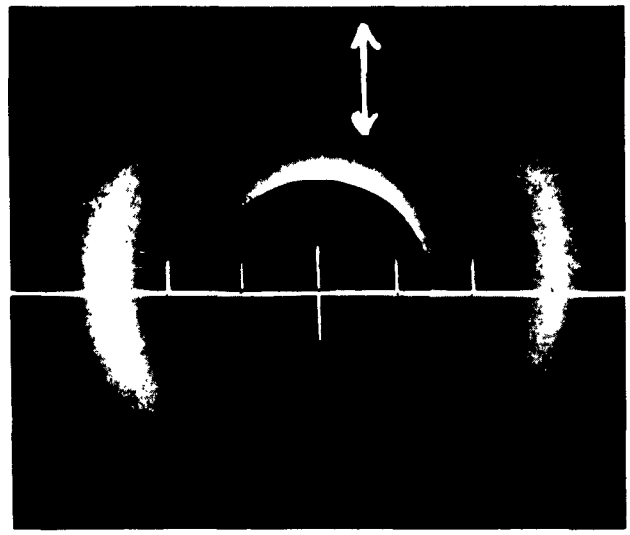

Fig. 27

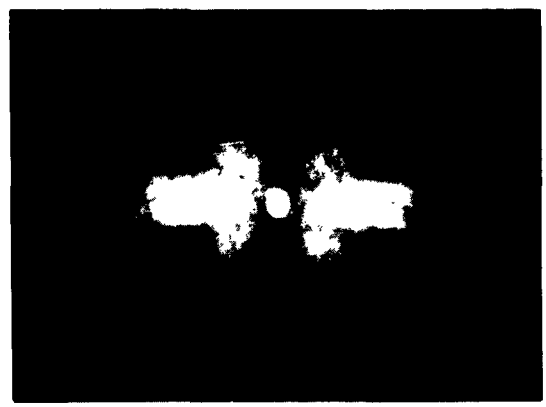

Fig. 28